

## Modification by ageing of the tetrodotoxin-sensitive sodium channels in rat skeletal muscle fibres

Jean-François Desaphy, Annamaria De Luca, Paola Imbrici, Diana Conte Camerino \*

*Unità di Farmacologia, Dipartimento Farmaco-Biologico, Facoltà di Farmacia, Università degli Studi di Bari, via Orabona 4, I-70125 Bari, Italy*

Received 16 February 1998; revised 7 May 1998; accepted 11 May 1998

### Abstract

Ageing leads to an impairment of muscle performance that may result from alteration of sarcolemma excitability. Therefore, we compare sodium channels of native fast-twitch skeletal muscle fibres of 21–26-month-old aged rats and 4–6-month-old young-adult rats, using the patch-clamp method. Extrajunctional sarcolemma of aged-rat fibres presented a higher sodium current density than that of young-rat fibres, which resulted from the presence of a higher number of available channels per membrane area. Open probability and availability voltage-dependence of sodium channels were similar in aged- and young-rat fibres, but permeation property was altered during ageing: aged-rat muscles showed a bimodal distribution of fibres with two values of sodium-channel conductance measured between  $-40$  and  $0$  mV; a young phenotype with a conductance close to  $18$  pS overlapping that found in young-rat fibres and an aged phenotype with a lower approximately half conductance. Current–voltage curves extended to  $-60$  and  $+20$  mV showed that the aged-phenotype conductance level resulted from an outward rectification occurring in these aged-rat fibres. Furthermore, in these aged-rat fibres belonging to the aged phenotype, ensemble average sodium currents showed slower activation and inactivation kinetics. Sodium currents of the two phenotypes were blocked by  $100$  nM tetrodotoxin, therefore excluding possible denervation effect. These age-related modifications in sodium current may contribute to the alteration of muscle excitability and function observed during the ageing process. © 1998 Elsevier Science B.V. All rights reserved.

**Keywords:** Aging; Sodium channel; Skeletal muscle; Patch clamp; Tetrodotoxin; (Rat)

### 1. Introduction

The process of ageing leads to profound impairments of muscle performance as decreases in muscle strength and speed of contraction. Factors underlying these impairments are complex, but intrinsic alterations within the muscle cell may play an important role [1]. A plausible origin of slowing

contraction may be the alteration of sarcolemma excitability that has been observed in current-clamp studies performed on aged-rat fast-twitch muscle [2,3]. The high chloride conductance that normally stabilises the resting membrane potential is reduced in aged rat sarcolemma, which leads to an increase in membrane resistance [2–4]. The activity of ATP-sensitive potassium channels declines in aged rats [5], but that of calcium-activated potassium channels increases with ageing [6], which results in enhanced macroscopic potassium conductance [2,3,6]. In addition, L-type calcium currents are reduced in ageing

\* Corresponding author. Fax: +39 (80) 544-2801;  
E-mail: conte@farmbiol.uniba.it

rat skeletal muscle [7]. All this suggests a broad alteration of channel protein function in the sarcolemma of aged subjects.

Voltage-gated sodium channels are responsible for the initial rise and subsequent conduction of action potential in skeletal muscle fibre [8]. Modification of sodium channel availability and behaviour is obviously a good candidate for alteration of action potential and then speed of contraction observed during ageing. Two sodium channel isoforms that are encoded by two different genes are expressed in skeletal muscle, depending on the differentiation and the innervation state [9,10]. During development, both *in vivo* and *in vitro*, the expression of the juvenile isoform SkM2 is gradually reduced and expression of the adult isoform SkM1 takes place [10,11]. After denervation, SkM2 is expressed *de novo* while expression of SkM1 is reduced [12,13]. SkM1 and SkM2 channels differ by their gating and their sensitivity to pharmacological agents [13–15]. Classically, nanomolar concentration of tetrodotoxin (TTX) blocks SkM1 channels whereas inhibition of SkM2 channels requires TTX concentration in the micromolar range. Nothing is known about the expression pattern of sodium channel isoforms during ageing but denervation and subsequent reinnervation of skeletal muscle fibres, which may induce modification of protein expression, have been proposed to occur during the ageing process [16,17]. In the present paper, we show that the density of TTX-sensitive sodium current is higher in fast-twitch skeletal muscle fibres of aged rats than in those of young rats. Sodium channels of aged-rat fibres showed open probability, voltage-dependence of availability, and TTX-sensitivity similar to those observed in young-rat fibres, but a population of aged-rat fibres presented sodium channels with altered permeation and kinetic properties.

## 2. Materials and methods

### 2.1. Muscle fibre preparation

Fibres from flexor digitorum brevis (FDB) muscles of the hind feet were obtained from young-adult rats (4–6 months, roughly estimated to be equivalent to 20–30 years in humans) and aged rats (21–26

months, approximately equivalent to 60–70 years in humans) as previously described [5]. Animals were killed either by an overdose of urethane (*i.p.* injection) or by decapitation. FDB muscles were promptly removed and placed in Ringer solution supplemented with 2.5–3 mg/ml collagenase (3.3 I.U./ml, type XI-S, Sigma, St Louis, MO, USA). They were shaken at 70 min<sup>-1</sup> for 1–2 h at 32°C under a 95% O<sub>2</sub>/5% CO<sub>2</sub> atmosphere. During this incubation, dissociated cells were sampled, rinsed several times with bath solution before being transferred to the RC-11 recording chamber (Warner Instrument, Hamden, CT, USA). Most of the fibres appeared intact with visible sarcomere cross-striation under an 400×-inverted microscope (Axiovert 100, Zeiss, Germany). However, some fibres isolated from aged rats appeared atrophied and were discarded.

### 2.2. Recording conditions

Single-channel currents were recorded at room temperature (21 ± 2°C) in the inside-out configuration of the patch-clamp method [18] with the Axo-Patch 1D amplifier and the CV-4-0.1/100 U headstage (Axon Instruments, Foster City, CA, USA). Pipettes were formed from Corning 7052 glass (Garner Glass, Claremont, CA, USA) with an automatic horizontal puller (DMZ universal puller, Zeitz Instruments, Augsburg, Germany). They were coated with Sylgard 184 (Dow Corning, Belgium) and heat polished on a microforge (MF-83, Narishighe, Tokyo, Japan). Chosen pipettes filled with the pipette solution had resistances ranging from 2.0 to 3.3 MΩ. Voltage-clamp protocols and data acquisition were performed with PClamp 6.0 software (Axon Instruments, Foster City, CA, USA) through a 12-bit AD/DA interface (digidata 1200, Axon Instruments, Foster City, CA, USA). Currents elicited by pulses at the frequency of 2 Hz were low-pass filtered at 2 kHz (–3 dB) by the amplifier four-pole Bessel filter and digitised at 40 kHz.

### 2.3. Data analysis

Subtracting the average of blank sweeps from the records eliminated capacity transients and leak currents. Single-channel current amplitudes (*i*) were measured on long (>1 ms) single-channel events

by direct inspection of traces. All-points amplitude histograms that we performed on some patches gave similar results. Single-channel conductance was calculated as the slope of the linear regression of single-current/voltage curves between  $-40$  and  $0$  mV. The density of sodium current ( $I_{\text{peak}}/\text{membrane area}$ ) was calculated by dividing the peak amplitude of ensemble average currents by the square of the pipette conductance that was assumed to be linearly correlated to the patch area. The density of available sodium channels ( $N/\text{membrane area}$ ) was calculated by dividing the maximal peak amplitude of currents elicited by depolarisations from  $-100$  to  $-20$  mV by  $i$  and the square of the pipette conductance. We considered only results obtained with pipette resistances ranging from  $2$  to  $3.3$  M $\Omega$  in order to limit the variation in patch membrane deformation under the pipette tip. Because sodium channel density is 5- to

10-fold higher on the end-plate border than away from the end plate [19], patches were performed at more than  $200$   $\mu\text{m}$  from the end plate. The voltage-dependence of sodium channel availability was studied on steady-state inactivation curves obtained by depolarising the patch to  $-20$  mV from various holding potentials (from  $-120$  to  $-70$  mV). Ensemble average currents were constructed from at least 200 test-pulses applied every  $0.5$  ms. The normalised peak current/holding potential relationships were fitted with the Boltzmann equation  $I/I_{\text{max}} = 1/\{1 + \exp[(V - V_{h1/2})/K]\}$  where  $V_{h1/2}$  is the potential for having half of the channels inactivated and  $K$  the slope factor. The open probability ( $P_o$ ) was calculated at  $-20$  mV by dividing the peak amplitude of ensemble average currents by  $iN$ . Fast kinetics of ensemble average sodium currents were studied at  $-40$  mV by measuring the time needed for current to reach

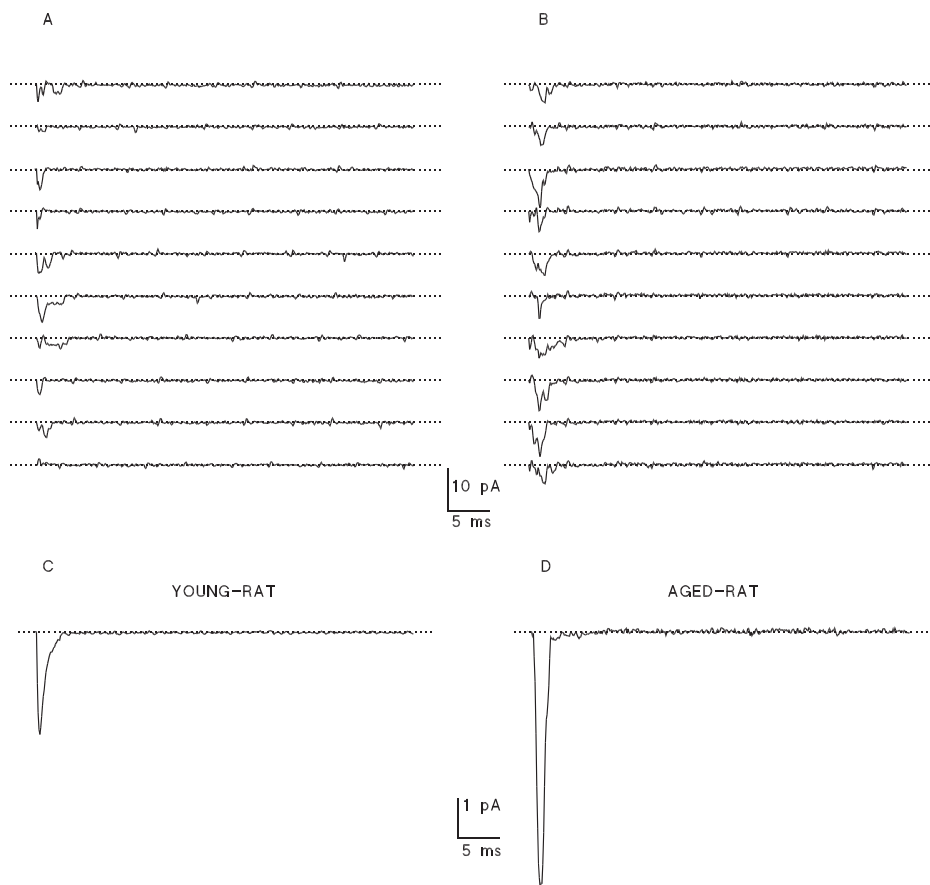


Fig. 1. Sodium channel recordings in skeletal muscle fibres of young and aged rats. (A,B) Ten consecutive traces of current elicited by voltage pulses of  $50$  ms duration, applied every  $0.5$  s, from  $-100$  to  $-20$  mV, in inside-out patches from young-rat fibres (A) and aged-rat fibres (B). Dashed lines show the zero-current level. (C,D) Ensemble average currents constructed from 400 traces elicited in the same patches as in (A) and (B), respectively.

its maximum (time-to-peak, TTP) and the time constant of the mono-exponential fit of the current decay phase ( $\tau$ ). To test the sensitivity of sodium channels to tetrodotoxin (TTX, Sigma, St Louis, MO, USA), we performed consecutively two or three cell-attached patches on a small-delimited area of each fibre from both young and aged rats. The pipette used for the first patch was filled with the control pipette solution. The pipette used for the second patch was filled with the same pipette solution supplemented with 100 nM TTX. To rule out the pos-

sibility of channel activity run-down between the first and the second patches, a third patch was performed on some fibres with the control pipette solution. All pipettes used for the different patches performed on each fibre were chosen to have closely the same diameter. The measurement of single-channel conductance in aged-rat fibres allowed us to discriminate between fibres belonging to the young and the aged phenotypes. To evaluate the effect of the toxin, the peak amplitude of ensemble average currents elicited by a depolarising pulse from  $-100$  to  $-20$  mV was

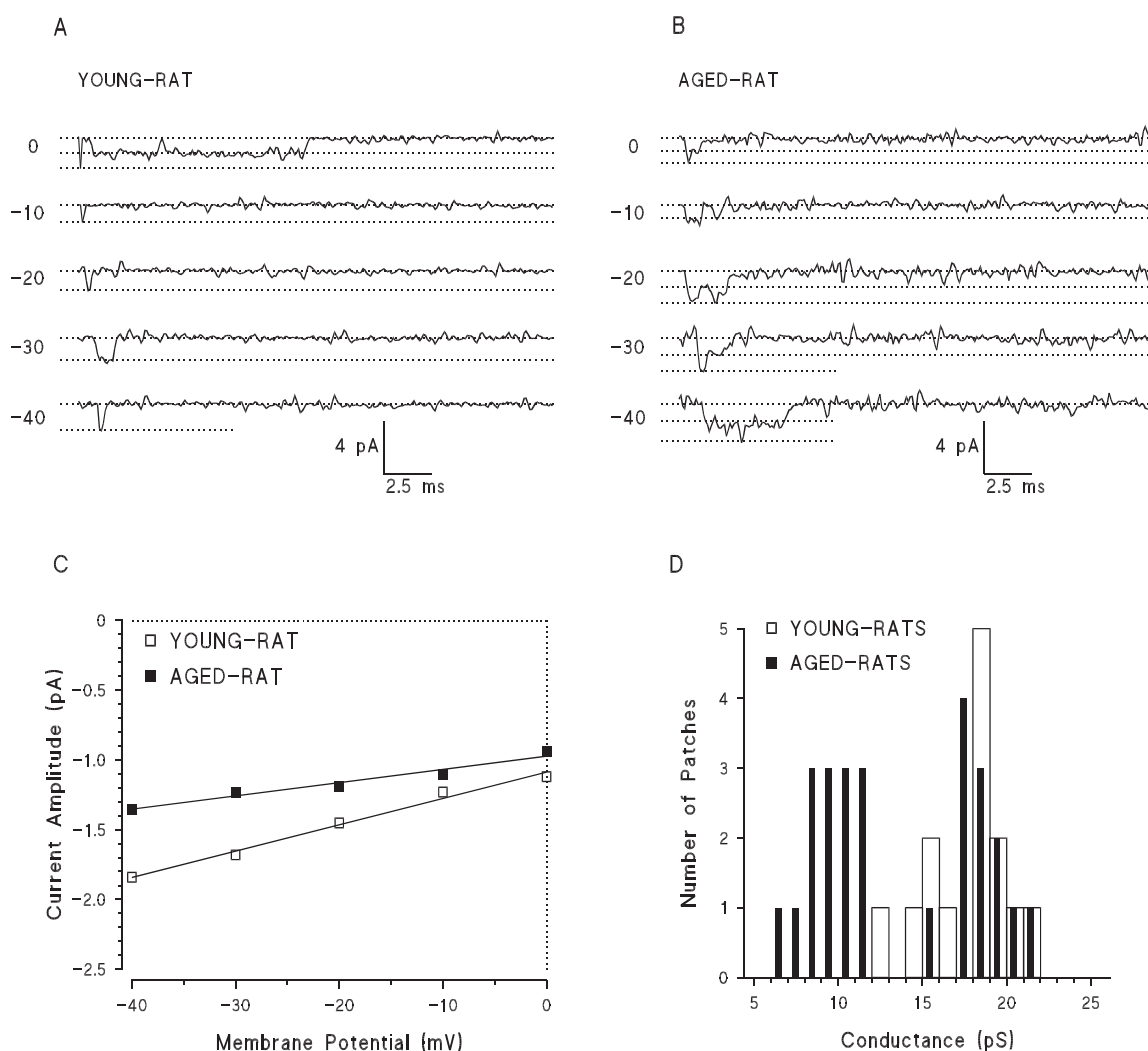


Fig. 2. Single-channel sodium conductance in skeletal muscle fibres of young and aged rats. (A,B) Openings of sodium channels elicited by depolarising the membrane to potentials ranging from  $-40$  to  $0$  mV in inside-out patches of young-rat (A) and aged-rat (B) fibres, which contained at least two and nine channels, respectively. (C) Single-channel conductances calculated as the slope of the linear regression were  $18.9$  pS for the patch in (A) and  $9.5$  pS for the patch in (B). (D) Sampled results show a monotone distribution of single-channel conductances in 10 young rats ( $17.6 \pm 0.7$  pS ( $n=14$  fibres)) and a bimodal distribution in 11 aged rats ( $18.7 \pm 0.5$  pS ( $n=12$ ) and  $9.6 \pm 0.4$  pS ( $n=14$ )).

measured in each patch and normalised with respect to the first patch (in the CsCl-enriched bath solution, the fibre membrane potential was close to  $-5$  mV).

Average results are done as mean  $\pm$  S.E. ( $n$  = number of fibres). Student's  $t$ -test were performed for grouped data with Fig. P 6.0 (Biosoft, Cambridge, UK).

## 2.4. Solutions

Ringer solution contained 145 mM NaCl, 5 mM KCl, 1 mM  $\text{MgCl}_2$ , 1 mM  $\text{CaCl}_2$ , 10 mM MOPS and 5 mM glucose. Bath solution contained 145 mM CsCl, 5 mM EGTA, 1 mM  $\text{MgCl}_2$ , 10 mM HEPES and 5 mM glucose. Pipette solution contained 150 mM NaCl, 1 mM  $\text{MgCl}_2$ , 1 mM  $\text{CaCl}_2$  and 10 mM HEPES. Both solutions were buffered at pH 7.3. The junction potential of about  $-5$  mV was not corrected.

## 3. Results

Membrane depolarisations elicited sodium channel openings in more than 90% of the patches of both young and aged rats. Both single openings and overlapping events occurred generally at the beginning of the test pulse (Fig. 1). Sometimes, long openings, late openings or reopenings were observed along the 50 ms-duration test pulse. Ensemble average currents showed the characteristics of sodium macroscopic currents with rapid onset and inactivation (Fig. 1). Interpulse duration of 0.45 s at  $-100$  mV allowed complete recovery from the inactivation that occurred at  $-20$  mV (not shown). In both young and aged rats, peak current amplitudes of ensemble average currents, recorded at  $-20$  mV and normalised in function of the pipette (see Section 2), were greatly variable from a fibre to another but the mean was significantly higher in fibres of aged rats ( $I_{\text{peak}} = 38.7 \pm 8.2$  pA/membrane area,  $n = 21$  fibres from 12 rats) than in those of young-adult rats ( $I_{\text{peak}} = 12.0 \pm 3.5$  pA/membrane area,  $n = 19$  fibres from 15 rats,  $P < 0.01$ ). Enhanced sodium current may result from a major single-channel conductance, a major number of available channels, or a major channel open probability.

Single-channel conductance was calculated as the

slope of linear regression of single-channel current/voltage ( $i$ - $V$ ) curves between  $-40$  and  $0$  mV (Fig. 2). It was  $17.6 \pm 0.7$  pS ( $n = 14$  fibres from 10 rats) in young-rat fibres (Fig. 2). In 11 aged rats, the conductance was distributed among two mean values which were  $18.7 \pm 0.5$  pS ( $n = 12$ ) and  $9.6 \pm 0.4$  pS ( $n = 14$ ). The latter was significantly smaller than the two others ( $P < 0.01$ ). Both types of conductance were observed in the same aged rat. We cannot exclude the presence of both types in the same fibre, but one always strongly predominated the other. Based on this result, we defined a 'young' phenotype constituted of aged-rat fibres presenting a conductance of about 18 pS, close to that observed in young-rat fibres, and an 'aged' phenotype constituted of aged-rat fibres presenting a conductance close to 9 pS.

The reversal potentials of  $i$ - $V$  curves were evaluated by extrapolation of the linear regression. Similar values were obtained in young-rat fibres ( $+52.8 \pm 4.7$  mV,  $n = 14$ ) and in aged-rat fibres of the young phenotype ( $+54.1 \pm 3.1$  mV,  $n = 12$ ,  $P = 0.82$ ). By contrast, the calculated reversal potential was significantly higher in aged-rat fibres of the

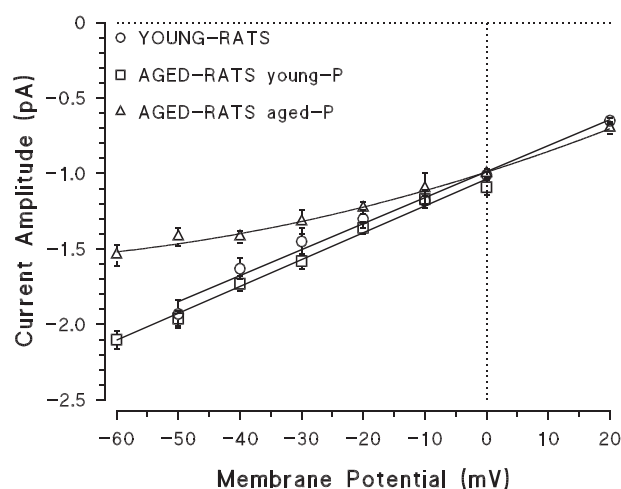


Fig. 3. Extended single-current/voltage curves of skeletal muscle sodium channels in young- and aged-rat fibres. Each data point is the mean  $\pm$  S.E. of single-channel amplitudes measured in three to thirteen inside-out patches. Curves for young-rat fibres and aged-rat fibres belonging to the young phenotype, as defined in text, are well fitted by a linear regression between  $-60$  and  $+20$  mV. The curve for the aged-rat fibres belonging to the aged phenotype is fitted by a polynomial regression of second order.

aged phenotype ( $+110.9 \pm 5.8$  mV,  $n = 14$ ,  $P < 0.001$ ). This suggested different ion selectivity between the two phenotypes or the presence of a voltage-dependent rectification.  $i$ - $V$  curves extended to  $-60$  and  $+20$  mV and calculated from combined data of each phenotype are represented in Fig. 3. While  $i$ - $V$  relationships for young-rat fibres and aged-rat fibres belonging to the young phenotype are quite linear between  $-60$  and  $+20$  mV, the  $i$ - $V$  relationship for aged-rat fibres belonging to the aged phenotype shows an outward rectification which may, at least in part, be responsible for the lower conductance measured at negative potentials.

The number of available channels was greatly variable from one patch to another (Fig. 4A), reflecting the well-known heterogeneous distribution of sodium channels on the sarcolemma [8]. However, aged-rat fibres belonging to the aged phenotype showed a significant higher mean number of available channels per membrane area at  $-100$  mV ( $79.1 \pm 12.2$ ,  $n = 12$  fibres from eight rats) than young-rat fibres ( $31.4 \pm 6.3$ ,  $n = 10$  fibres from eight rats,  $P < 0.005$ ). Aged-rat fibres belonging to the young phenotype presented an intermediary situation ( $52.4 \pm 9.8$ ,  $n = 8$  fibres from four rats,  $P = 0.097$  versus young-rat fibres,  $P = 0.106$  versus aged-rat fibres of aged phenotype). The voltage-dependence of steady-state inactivation did not significantly differ between fibres of young and aged rats (Fig. 4B). The potentials for having half of the channels inactivated  $V_{h1/2}$ , deter-

mined as described in the methods, were  $-105.0 \pm 1.5$  mV ( $n = 4$ ) and  $-101.7 \pm 1.5$  mV ( $n = 7$ ,  $P = 0.190$ ) while the slope factors  $K$  of the Boltzmann distribution were  $4.0 \pm 0.6$  ( $n = 4$ ) and  $4.7 \pm 0.3$  ( $n = 7$ ,  $P = 0.291$ ) in young- and aged-rat fibres, respectively. This suggests that the higher number of available channel that we observed at  $-100$  mV in aged-rat fibres results from a greater number of physical sodium channels in the sarcolemma.

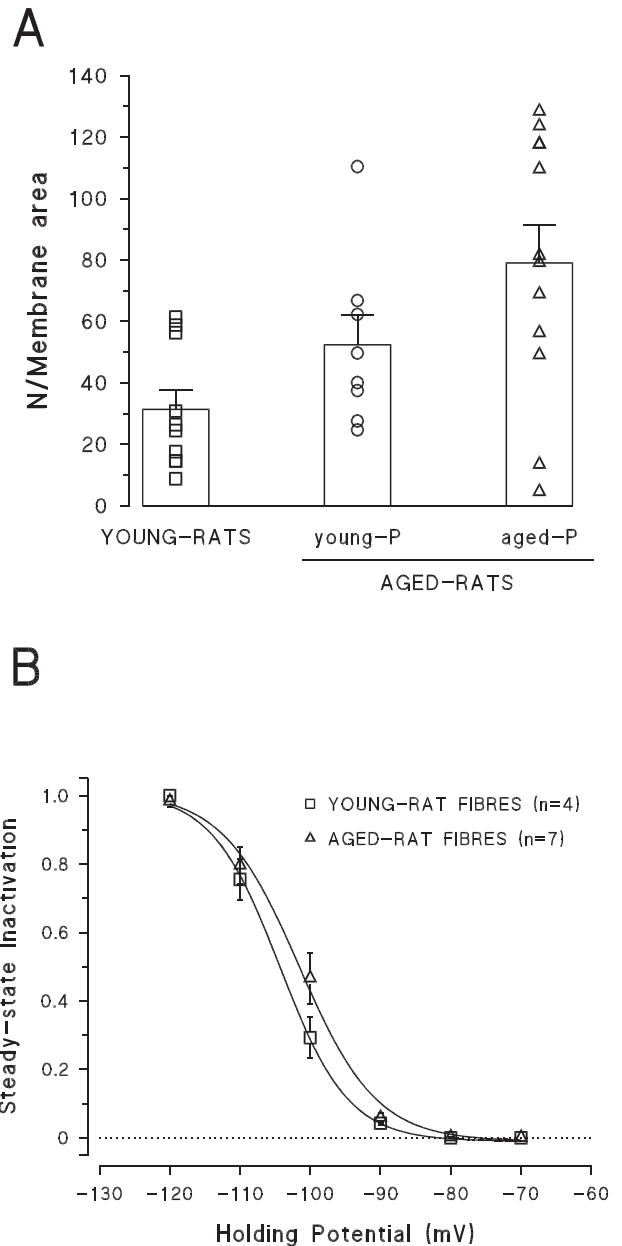


Fig. 4. Availability of sodium channels in skeletal muscle fibres of young and aged rats. (A) The number of available channels ( $N$ ) per membrane area at  $-100$  mV was calculated by dividing the maximum peak amplitude of currents elicited at  $-20$  mV from a holding potential of  $-100$  mV by the square of pipette conductance. Symbols give individual values and bars represent the mean  $\pm$  S.E. The channel density of aged-rat fibres belonging to the aged phenotype, as defined in the text, is significantly higher than that of young-rat fibres ( $P < 0.005$ ). (B) The voltage dependence of channel availability was deduced from steady-state inactivation curves of sodium channels in skeletal muscle fibres of young and aged rats. The patch membrane was depolarised every  $0.5$  s to  $-20$  mV from various holding potentials (from  $-120$  to  $-70$  mV). The mean  $\pm$  S.E. of ensemble average peak currents, normalised with respect to the maximum one measured at  $-120$  or  $-110$  mV, is plotted as a function of the holding potential. Experimental data points are fitted with the Boltzmann equation as described in Section 2.

Open probability at  $-20$  mV was not significantly different between all fibre types (Fig. 5). It was  $0.35 \pm 0.09$ ,  $0.40 \pm 0.06$ , and  $0.31 \pm 0.07$  in young-rat fibres, aged-rat fibres of the young phenotype, and aged-rat fibres of the aged phenotype, respectively.

Ensemble average sodium currents of aged-rat fibres belonging to the young phenotype showed fast kinetics similar to those of young-rat fibres (not shown). By contrast, sodium currents of aged-rat fibres belonging to the aged phenotype activated and inactivated slower at  $-40$  mV than those of young-rat fibres (Fig. 6). The time needed for sodium current to reach the peak at  $-40$  mV was  $0.93 \pm 0.11$  ms ( $n=7$ ) and  $3.69 \pm 1.10$  ms ( $n=7$ ,  $P<0.05$ ) for young-rat fibres and aged-rat fibres belonging to the aged phenotype, respectively. The decay time constant at  $-40$  mV, calculated by fitting current inactivation with a mono-exponential, was  $1.06 \pm 0.22$  ms ( $n=7$ ) and  $2.43 \pm 0.47$  ms ( $n=7$ ,  $P<0.05$ ) for young-rat fibres and aged-rat fibres belonging to the aged phenotype, respectively.

To test the sensitivity of sodium channels to TTX,

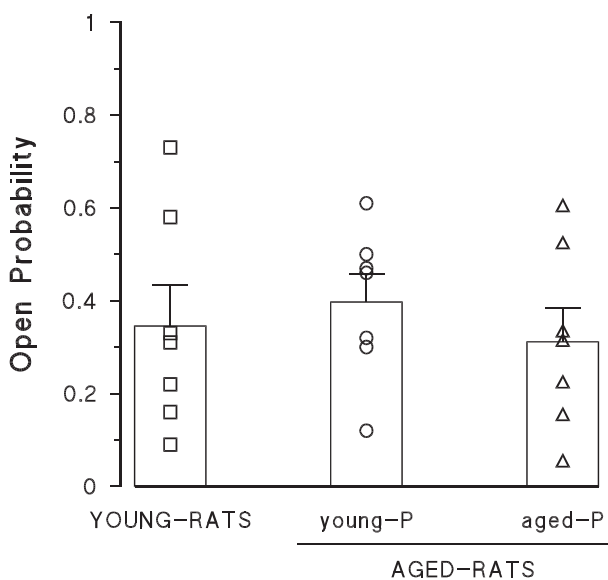


Fig. 5. Open probability of sodium channels at  $-20$  mV in skeletal muscle fibres of young and aged rats. The open probability  $P_o$  was calculated at  $-20$  mV by dividing the peak amplitude of ensemble average currents by  $iN$ . Symbols give individual values and bars represent the mean  $\pm$  S.E. No significant difference was found.

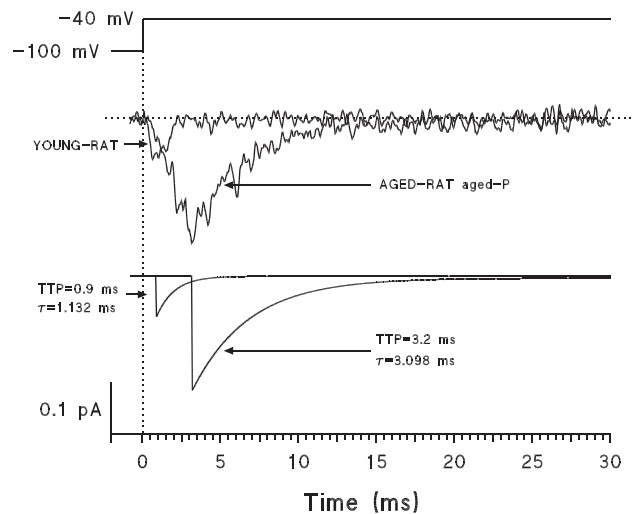


Fig. 6. Fast kinetics of sodium currents at  $-40$  mV in skeletal muscle fibres of young and aged rats. Ensemble average sodium currents were constructed from at least 200 current traces elicited from  $-100$  to  $-40$  mV, every second. Upper traces show two representative sodium currents recorded in inside-out patches of a young-rat fibre and an aged-rat fibre belonging to the aged phenotype. The young-rat fibre patch contained at least two channels with a conductance of 18.1 pS, whereas the aged-rat fibre contained at least 10 channels with a conductance of 7.4 pS. Lower traces show exponential fits of inactivation of the same currents. Time to peak (TTP) and decay time constant ( $\tau$ ) measured in aged-rat fibres belonging to the aged phenotype were longer than those measured in young-rat fibres.

we consecutively performed two or three cell-attached patches on young-rat fibres, aged-rat fibres belonging to the young phenotype and aged-rat fibres belonging to the aged phenotype (Fig. 7). The first and third patches were performed in absence of TTX whereas the pipette solution used for the second patches contained 100 nM TTX (see Section 2). The currents recorded in the presence of 100 nM TTX were 5.6, 8.0, and 1.5% of the currents recorded in the first patch for young-rat fibres ( $n=3$ ), aged-rat fibres belonging to the young phenotype ( $n=2$ ), and aged-rat fibres belonging to the aged phenotype ( $n=2$ ), respectively. In the third patch (performed on four fibres), current amplitude was always higher than that measured in the presence of TTX, demonstrating that the smaller current recorded in the presence of TTX was not due to a run-down of channel activity between the first and the second patch.



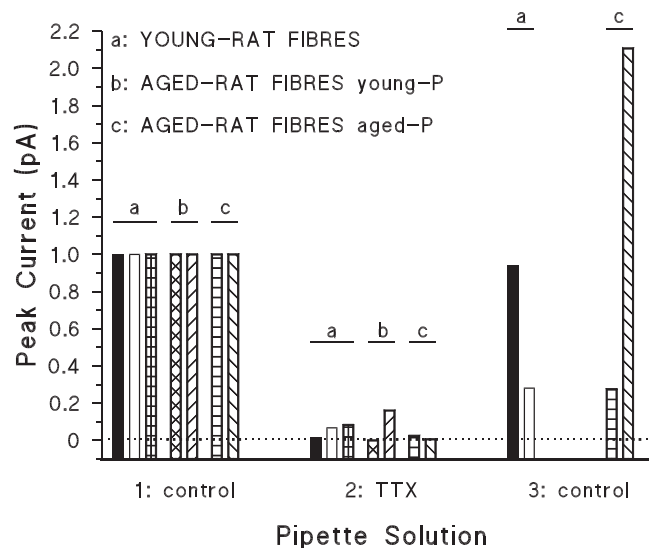


Fig. 7. Effects of 100 nM tetrodotoxin on sodium currents of skeletal muscle fibres of young and aged rats. Two or three cell-attached patches were performed on a small delimited area of the same fibre with (second patch) or without (first and third patches) 100 nM TTX in the pipette. The two or three pipettes used on each fibre were chosen to have closely the same diameter. Each bar-filling pattern corresponds to one fibre. Each bar represents the peak amplitude of ensemble average currents elicited in each patch by a depolarising pulse from  $-100$  to  $-20$  mV and normalised with respect to that found in the first patch.

#### 4. Discussion

##### 4.1. Functional significance of differences in sodium currents between young- and aged-rat muscle fibres

Performing voltage-clamp recordings on inside-out patches of extrajunctional membrane of freshly dissociated skeletal muscle fibres, we found a higher mean density of sodium current in aged-rat fibres than in young-adult rat fibres. Functionally, this could suggest higher muscle excitability and a lower resistance to fatigue of aged rats. For example, in hyperkalaemic periodic paralysis, an inherited muscle disorder due to mutations in the gene encoding the skeletal muscle sodium channel, an increased sodium current is responsible for sarcolemma over-excitability and muscle weakness [20]. During the ageing process, the increase in sodium current, together with the reported decreased chloride conductance in aged rat [2,3], should contribute to lower the threshold stimulation necessary to initiate the action potential as it has been observed in current-clamp studies performed on aged-rat fast-twitch muscle fibres [2,3]. Nevertheless, an increased influx of sodium ions, together with the increased potassium conductance [2,3] due to an increased activity of calcium-activated

potassium channel [6], would promote and accelerate accumulation of potassium ions in the transverse tubular system, reducing the firing capacity of aged-rat fibres as it has been observed in current clamp studies [2,3]. The slowing of sodium-current fast kinetics that we observed in aged-rat fibres of aged-phenotype may also contribute to the age-related reduction of firing capacity. In addition, an increased entry of sodium ions in the aged-muscle fibres would in turn decrease calcium extrusion through the sodium/calcium exchange. Such a mechanism might increase the duration of higher levels of cytosolic calcium in aged-muscle fibres, therefore contributing to the reduced twitch relaxation rate observed in aged muscle [21]. So combined modifications of chloride, potassium, and sodium permeabilities of the sarcolemma may account for membrane excitability alteration and, together with the reported modification of calcium channel function [22], for the subsequent perturbation of contraction occurring in aged subjects.

##### 4.2. Origin of the higher sodium current density in aged-rat muscle fibres

A higher sodium current density can result from a higher single-channel conductance, a higher open



probability, or a higher number of available channels. We found that open probability was not altered during ageing. The single sodium-channel conductance is either unchanged or reduced in aged-rat fibres. By contrast, the number of available channels per membrane area at  $-100$  mV was greater in aged-rat fibres. As voltage-dependence of steady-state inactivation was not modified, this would suggest a greater insertion of sodium channels in extrajunctional sarcolemma of aged-rat fibres. After denervation, an increase in total sodium-channel mRNA synthesis has been reported [23] together with the appearance of the juvenile sodium channel isoform SkM2 characterised by low-conductance level and low sensitivity to TTX [12,13]. However, sodium currents are highly sensitive to TTX in aged-rat fibres, therefore excluding a possible effect of age-related denervation in our study. The FDB muscle is a fast-twitch oxidative-glycolytic skeletal muscle that mostly contains fibres of type IIa [24]. It has been suggested that during ageing, transformation of muscle fibres from fast- to slow-twitch muscle type may occur in response to specific reinnervation [17]. It is unlikely to be the case in our study because rat slow-twitch muscle fibres has been shown to present less sodium current than fast-twitch muscle fibres [19]. Thus the enhanced channel density in aged-rat muscle fibre may be rather due to the age-related alteration of protein synthesis intrinsic to the muscle cell [1] and leading to an increased sodium channel expression. Another plausible explanation may be the potential redistribution of sodium channels along the membrane in response to the reported reorganisation of the sarcolemma observed during the ageing process [25]. A recent study reported an ageing-dependent and hypercholesterolaemia-related reduction of sodium current density, measured by means of the whole-cell patch-clamp technique in cardiac myocytes of rabbits [26]. However, heart and skeletal muscle sodium channels are encoded by different genes. Therefore, such a difference may reflect a tissue specificity of ageing-effect on sodium channels. In support of this, the effect of ageing on calcium channels also differs between skeletal muscle and heart, since a reduction of calcium current density was reported in aged skeletal muscles [7,22] whereas no change was noted in rat ventricular myocytes [27]. Moreover, while whole-cell recordings give a meas-

ure of the sodium current density for the total cell membrane, independently of the distribution of sodium channels on the myocyte surface, our cell-attached recordings are specifically restricted to the extrajunctional sarcolemma. Both technical approaches would be of interest to obtain more precise information but, unfortunately, the whole-cell patch-clamp method cannot be applied to the native skeletal muscle fibre because of the problem of space clamp. All this, together with the use of different animals of different ages in the study of Wu and colleagues and in ours, make the comparison between the results difficult.

#### 4.3. *Modification of single-channel sodium conductance and ensemble average sodium current fast kinetics in aged rat muscle fibres*

Based on single-channel sodium conductance measured between  $-40$  and  $0$  mV, we defined a young phenotype and an aged phenotype of skeletal muscle fibres of aged rats. The young phenotype showed a conductance of about  $18$  pS similar to that of the adult isoform of skeletal muscle sodium channels, found in the present study and by others in similar condition [28]. The aged phenotype with a conductance of about  $9$  pS was found in about half of the aged-rat fibres (54% of the fibres). The aged-phenotype low conductance level may be due to the outward rectification of the  $i-V$  curve, although we cannot exclude a modification in channel selectivity. Moreover, ensemble average sodium currents of aged-rat fibres belonging to the aged phenotype activated and inactivated slower than those of young-rat fibres and aged-rat fibres belonging to the young phenotype. Nevertheless, sodium currents of both phenotypes were blocked by  $100$  nM TTX. Thus, the two phenotypes may result from the expression of two isoforms of TTX-sensitive sodium channels encoded by two different genes. It has been reported that the mRNAs for rat neuronal type I and III sodium channels may represent 5% of the total sodium channel mRNAs expressed in the skeletal muscle of young-adult rats [29]. Although no evidence has been given yet for the possible expression of the corresponding channel proteins, variations in the amount of expressed neuronal-type sodium channels might occur in aged muscles. On the other hand,

a unique TTX-sensitive sodium channel, modified by the ageing process, may account for both phenotypes. Such modification may reside in the channel protein itself. For example, it has been demonstrated that external divalent cations can block sodium permeation, inducing an outward rectification, and can modify channel gating [30–33] and that the level of sialylation of the channel protein influences the sensitivity to external cations [34]. Thus a modification of the post-translational maturation of the channel  $\alpha$ -subunit in some aged-rat fibres may be responsible for the occurrence of the aged phenotype. On the other hand, a modification in the channel-surrounding lipid bilayer may occur during ageing [35,36], that may influence permeation and gating properties of sodium channels [37–39].

## Acknowledgements

The authors thank Dr. Sabata Pierno for her help in the course of this study. This work was supported by E.C. Contract C11\*-CT94-0037 and by the Italian C.N.R. Grants 95.0825 and 95.01000.PF 40 (Invecchiamento).

## References

- [1] E. Carmeli, A.Z. Reznick, *Proc. Soc. Exp. Biol. Med.* 262 (1994) 103–113.
- [2] A. De Luca, M. Mambrini, D. Conte Camerino, *Pflügers Arch.* 415 (1990) 642–644.
- [3] A. De Luca, S. Pierno, D. Cocchi, D. Conte Camerino, *J. Pharmacol. Exp. Ther.* 269 (1994) 948–953.
- [4] A. De Luca, D. Tricarico, S. Pierno, D. Conte Camerino, *Pflügers Arch.* 427 (1994) 80–85.
- [5] D. Tricarico, D. Conte Camerino, *Mol. Pharmacol.* 46 (1994) 754–761.
- [6] D. Tricarico, R. Petrucci, D. Conte Camerino, *Pflügers Arch.* 434 (1997) 822–829.
- [7] M. Renganathan, W.E. Sonntag, O. Delbono, *Biochem. Biophys. Res. Commun.* 235 (1997) 784–789.
- [8] B. Hille, *Ion Channels of Excitable Membranes*, Sinauer Associates, Sunderland, MA, 1984.
- [9] J.S. Trimmer, S.C. Cooperman, S.A. Tomiko, J. Zhou, S.M. Crean, M.B. Boyle, R.G. Kallen, Z. Sheng, R.L. Barchi, F.J. Sigworth, R.H. Goodman, W.S. Agnew, G. Mandel, *Neuron* 3 (1989) 33–49.
- [10] R.G. Kallen, Z.-H. Sheng, J. Yang, L. Chen, R.B. Rogart, R.L. Barchi, *Neuron* 4 (1990) 233–242.
- [11] C. Frelin, H.P.M. Vijverberg, G. Romey, P. Vigne, M. Lazdunski, *Pflügers Arch.* 402 (1984) 121–128.
- [12] J.S.-J. Yang, J.T. Sladky, R.G. Kallen, R.L. Barchi, *Neuron* 7 (1991) 421–427.
- [13] P.A. Pappone, *J. Physiol. (Lond.)* 306 (1980) 377–410.
- [14] R.E. Weiss, R. Horn, *Science* 233 (1986) 361–364.
- [15] M.M. White, L. Chen, R. Klenfield, R.G. Kallen, R.L. Barchi, *Mol. Pharmacol.* 39 (1991) 604–608.
- [16] E. Gutmann, V. Hanzlikova, *Adv. Behav. Res.* 16 (1975) 196–207.
- [17] F.P. Pettigrew, P.F. Gardiner, *Mech. Aging Dev.* 40 (1987) 243–259.
- [18] O.P. Hamill, A. Marty, E. Neher, B. Sakmann, F.J. Sigworth, *Pflügers Arch.* 391 (1981) 85–100.
- [19] R.L. Ruff, *Am. J. Physiol.* 262 (1992) C229–C234.
- [20] S.C. Cannon, *Neuromusc. Disord.* 7 (1997) 241–249.
- [21] R.C. Carlsen, D.A. Walsh, *Pflügers Arch.* 408 (1987) 224–230.
- [22] O. Delbono, K.S. O'Rourke, W.H. Ettinger, *J. Membr. Biol.* 148 (1995) 211–222.
- [23] S.S. Cooperman, S.A. Grubman, R.L. Barchi, R.H. Goodman, G. Mandel, *Proc. Natl. Acad. Sci. USA* 84 (1987) 8721–8725.
- [24] R.C. Carlsen, D. Larson, D.A. Walsh, *Can. J. Physiol. Pharmacol.* 63 (1985) 958–965.
- [25] E. Gutmann, V. Hanzlikova, F. Vyskocil, *J. Physiol. (Lond.)* 271 (1971) 331–343.
- [26] C.C. Wu, M.J. Su, J.F. Chi, M.H. Wu, Y.T. Lee, *Life Sci.* 61 (1997) 1539–1551.
- [27] K.E. Walker, E.G. Lakatta, S.R. Houser, *Cardiovasc. Res.* 27 (1993) 1968–1977.
- [28] R.L. Ruff, *Am. J. Physiol.* 271 (1996) C971–C981.
- [29] K.L. Schaller, D.M. Krzemien, N.M. McKenna, J.H. Caldwell, *J. Neurosci.* 12 (1992) 1370–1381.
- [30] S. Cukierman, B.K. Krueger, *Pflügers Arch.* 416 (1990) 360–367.
- [31] M. Chahine, L.-Q. Chen, R.G. Kallen, R.L. Barchi, R. Horn, *Biophys. J.* 62 (1992) 37–40.
- [32] R.J. French, J.F. Worley, W.F. Wonderlin, A.S. Kularatna, B.K. Krueger, *J. Gen. Physiol.* 103 (1994) 447–470.
- [33] P. Backx, D. Yue, J. Lawrence, E. Marban, G. Tomaselli, *Science* 257 (1992) 248–251.
- [34] E. Bennett, M.S. Urcan, S.S. Tinkle, A.G. Koszowski, S.R. Levinson, *J. Gen. Physiol.* 109 (1997) 327–343.
- [35] M. Shinitzky, *Gerontology* 33 (1987) 149–154.
- [36] E. Alvarez, V. Ruiz-Gutierrez, C. Santa Maria, A. Machado, *Mech. Ageing Dev.* 71 (1993) 1–12.
- [37] S. Cukierman, W.C. Zinkand, R.J. French, B.K. Krueger, *J. Gen. Physiol.* 92 (1988) 431–447.
- [38] C.C. Park, Z. Ahmed, *Brain Res.* 570 (1992) 75–84.
- [39] S. Ji, J.N. Weiss, G.A. Langer, *J. Gen. Physiol.* 101 (1993) 355–375.